Biosci. Biotechnol. Biochem., **75** (8), 1557–1563, 2011

Calcium Ion-Dependent Increase in Thermostability of Dextran Glucosidase from *Streptococcus mutans*

Momoko KOBAYASHI, Hironori HONDOH,* Haruhide MORI, Wataru SABURI, Masayuki OKUYAMA, and Atsuo KIMURA†

Research Faculty of Agriculture, Hokkaido University, Kita-9 Nishi-9 Kita-ku, Sapporo 060-8589, Japan

Received April 1, 2011; Accepted May 16, 2011; Online Publication, August 7, 2011
[doi:10.1271/bbb.110256]

Dextran glucosidase from *Streptococcus mutans* (SmDG), which belongs to glycoside hydrolase family 13 (GH13), hydrolyzes the non-reducing terminal glucosidic linkage of isomaltooligosaccharides and dextran. Thermal deactivation of SmDG did not follow the single exponential decay but rather the two-step irreversible deactivation model, which involves an active intermediate having 39% specific activity. The presence of a low concentration of $CaCl_2$ increased the thermostability of SmDG, mainly due to a marked reduction in the rate constant of deactivation of the intermediate. The addition of $MgCl_2$ also enhanced thermostability, while KCl and NaCl were not effective. Therefore, divalent cations, particularly Ca^{2+}, were considered to stabilize SmDG. On the other hand, $CaCl_2$ had no significant effect on catalytic reaction. The enhanced stability by Ca^{2+} was probably related to calcium binding in the $\beta \rightarrow \alpha$ loop 1 of the $(\beta/\alpha)_8$ barrel of SmDG. Because similar structures and sequences are widespread in GH13, these GH13 enzymes might have been stabilized by calcium ions.

Key words: dextran glucosidase; thermostability; two-step irreversible deactivation; calcium-binding site; glycoside hydrolase family 13

Dextran glucosidase, found in *Streptococcus mutans* (SmDG) as the *dex*B gene product, hydrolyzes $(1 \rightarrow 6)$-α-D-glucosidic linkages at the non-reducing end of substrates to release glucose.[1)] The enzyme acts preferably on short-chain isomaltooligosaccharides, but also hydrolyzes dextran.[1,2)] SmDG catalyzes transglucosylation at high concentrations of the substrate, resulting in the formation of α-1,6-glucosidic linkages.[2)]

Glycoside hydrolases are classified into glycoside hydrolase families on the basis of sequence similarity. The largest group in the CAZy database (http://www.cazy.org)[3)] is glycoside hydrolase family 13 (GH13), which contains α-amylase, cyclodextrin glucanotransferase, α-glucosidase, and many different activities in addition to dextran glucosidase. Most GH13 enzymes act on α-glycosides, such as starch, glycogen, and related oligo- and polysaccharides, and catalyze predominantly hydrolysis and transglycosylation with retention of the α-anomeric configuration. GH13 enzymes share a core three-domain structure composed of domains A, B, and C. Domain A is a $(\beta/\alpha)_8$ barrel fold, domain B is a long protruding loop between $\beta 3$ and $\alpha 3$ in the $(\beta/\alpha)_8$ barrel, and domain C is an antiparallel β-sheet at the C-terminus. The catalytic center, subsite -1, is structurally well-conserved by seven invariant amino acid residues, while the other parts are structurally diverse so that the enzymes catalyze different reactions.[4)] GH13 enzymes are classified into 36 subfamilies on the basis of amino acid sequence.[5)] Dextran glucosidase belongs to subfamily 31 (GH13_31), together with oligo-1,6-glucosidase, α-glucosidase, sucrose isomerase, isomaltulose synthase, and trehalulose synthase. The enzymes act on α-glucoside at the non-reducing ends of the substrates, and catalyze hydrolysis, transglucosylation, and isomerization.

Some GH13 enzymes require calcium ions for activity and stability. In particular, the most predominant α-amylases are dependent on calcium ions.[6)] Many α-amylases possess two calcium-binding sites in domain B, and the bound calcium ions stabilize the protruding loop structure.[7)] Other GH13 enzymes, such as cyclodextrin glucanotransferase, cyclodextrinase, and α-glucosidase, are also calcium dependent,[8–11)] and possess Ca^{2+} in the equivalent positions and/or different parts of the structures.[12–23)] Trehalulose synthase, a member of subfamily GH13_31, has one calcium ion in the $\beta \rightarrow \alpha$ loop 1.[13)] In cyclodextrin glucanotransferase[8)] and α-amylase 2 (TVAII) of *Thermoactinomyces vulgaris*,[22)] calcium ions function to enhance the stability.

SmDG is one of the enzymes containing Ca^{2+} in the solved structures.[12)] It has a simple three-domain architecture, and the $\beta \rightarrow \alpha$ loops of domain A and part of domain B are involved in the formation of a pocket-shaped active site, in which the residues in subsite -1 are conserved structurally at the bottom. On the outside of the active pocket, one calcium ion is coordinated tightly by atoms of Asp21, Asn23, Asp25, Ile27, and Asp29 in the $\beta \rightarrow \alpha$ loop 1 of domain A (Fig. 1).[12)]

In this report, we present the denaturation kinetics of SmDG. The denaturation of proteins is generally described by a single-step irreversible denaturation model, in which denaturation is expressed by a single rate constant. Another model is the two-step irreversible

† To whom correspondence should be addressed. Tel/Fax: +81-11-706-2808; E-mail: kimura@abs.agr.hokudai.ac.jp
* Present address: *Graduate School of Biosphere Science, Hiroshima University, 1-4-4 Kagamiyama, Higashi-Hiroshima 739-8528, Japan*

Abbreviations: BSA, bovine serum albumin; CGTase, cyclodextrin glucanotransferase; GH, glycoside hydrolase; pNP, *p*-nitrophenol; pNPG, *p*-nitrophenyl α-glucopyranoside; SmDG, dextran glucosidase from *Streptococcus mutans* model, in which an irreversible active intermediate is postulated before the enzyme is completely inactivated.[24] This model has been used to describe the thermal denaturation of *Bacillus licheniformis* α-amylase,[24] and has been employed for other enzymes.[25,26] We applied the two-step irreversible denaturation model to evaluate the thermostability of SmDG and to investigate the effect of calcium ions on thermostability. The thermal denaturation was described well by the model, and the presence of Ca^{2+} enhanced thermostability. Increased stability with the calcium ion is a novel characteristic of GH13_31 enzymes. The possibility that many enzymes belonging to several GH13 subfamilies have the similar properties is discussed.

Materials and Methods

Enzyme. Recombinant His_6-tagged SmDG was prepared as described previously.[2] It was produced in *Escherichia coli* BL21(DE3) CodonPlus RIL (Stratagene, La Jolla, CA, USA) transformant harboring the expression plasmid derived from pET23d (Novagen, Darmstadt, Germany) and purified to homogeneity through a Ni-chelating Sepharose column (Chelating Sepharose FastFlow; GE Healthcare, Little Chalfont, UK). The purified enzyme was dialyzed thoroughly against 20 mM sodium acetate buffer (pH 6.0) and 0.02% sodium azide.

Biochemical assay. The protein concentration was determined by quantification of the various amino acids by the ninhydrin colorimetric method using an amino acid analyzer (JEOL model JLC-500/V, Tokyo, Japan) after hydrolysis of 26 µg of SmDG in 6 M HCl at 110 °C for 24 h.[27]

Enzyme activity (1 U) was defined as the amount of enzyme that catalyzes the release of *p*-nitrophenol (pNP) at an initial rate of 1 µmol s^{-1} from 2 mM *p*-nitrophenyl α-glucopyranoside (pNPG; Nacalai Tesque, Kyoto, Japan) under standard reaction conditions. The reaction mixture (50 µL), composed of 2 mM pNPG, 40 mM sodium acetate buffer (pH 6.0), 0.02% bovine serum albumin (BSA), 0.02% sodium azide, and an adequate concentration of SmDG, was incubated at 37 °C for 10 min. The enzymatic reaction was stopped by the addition of 100 µL of 1 M Na_2CO_3, and liberated pNP was calculated from A_{400} of the mixture using $\varepsilon_{1\,\mathrm{mM},\,400\,\mathrm{nm}} = 16.7$, which was experimentally obtained. To determine the catalytic parameters, the enzymatic reaction mixture (250 µL) was formulated to contain 0.2–12 mM pNPG and 1.2 mM EDTA in addition to 40 mM sodium acetate buffer (pH 6.0), 0.02% BSA, 0.02% sodium azide, and SmDG. To quantitate liberated pNP, 100 µL of the mixture was withdrawn and mixed with 200 µL of 1 M Na_2CO_3. To measure glucose concentrations, the enzyme reaction (100 µL) was terminated by the addition of 50 µL of 4 M Tris–HCl buffer (pH 7.0), and glucose was quantified by the glucose oxidase-peroxidase method[28] using Glucose CII Test Wako (Wako Pure Chemical Industries, Osaka, Japan).

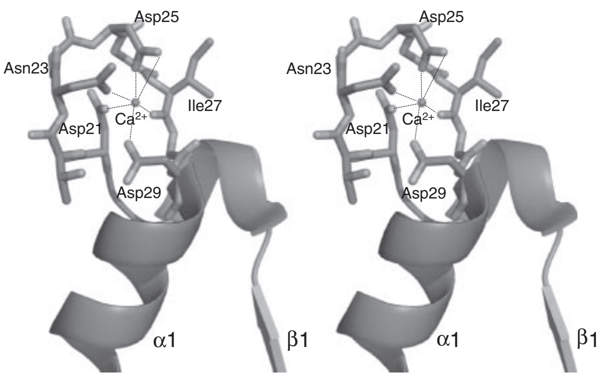

Fig. 1. A Calcium Ion Situated in $\beta \rightarrow \alpha$ Loop 1 in the $(\beta/\alpha)_8$ Barrel Structure of SmDG[12] (Stereo View).

A calcium ion interacts with five atoms of side chains (Asp21 OD1, Asn23 OD1, Asp25 OD1 and OD2, and Asp29 OD2), one carbonyl oxygen of the main chain (Ile27), and two water molecules (not shown). The strand with β1 and the helix with α1 indicate β-strand 1 and α-helix 1 in the catalytic $(\beta/\alpha)_8$ barrel, respectively.

Kinetic parameters of catalytic reaction. The reaction scheme shown in Fig. 2 gave rise to equations of reaction velocities of aglycone-release (v_{ag}), hydrolysis (v_h), and transglucosylation (v_{tg}) expressed as a function of the substrate concentration ([S]):[29,30]

$$v_{ag} = (k_{cat2}[S]^2 + k_{cat1}K_{m2}[S])/([S]^2 + K_{m2}[S] + K_{m1}K_{m2}) \tag{1}$$

$$v_h = k_{cat1}K_{m2}[S]/([S]^2 + K_{m2}[S] + K_{m1}K_{m2}) \tag{2}$$

$$v_{tg} = k_{cat2}[S]^2/([S]^2 + K_{m2}[S] + K_{m1}K_{m2}) \tag{3}$$

where kinetic parameters, k_{cat1}, k_{cat2}, K_{m1}, and K_{m2}, were defined as follows by the rate constants shown in Fig. 2:

$$K_{m1} = k_3(k_{-1} + k_2)(k_{-4} + k_5)/\{k_4k_5(k_{-1} + k_2) + k_1(k_{-4} + k_5)(k_2 + k_3)\}$$

$$K_{m2} = \{k_4k_5(k_{-1} + k_2) + k_1(k_{-4} + k_5)(k_2 + k_3)\}/k_1k_4(k_2 + k_5)$$

$$k_{cat1} = k_1k_2k_3(k_{-4} + k_5)/\{k_4k_5(k_{-1} + k_2) + k_1(k_{-4} + k_5)(k_2 + k_3)\}$$

$$k_{cat2} = k_2k_5/(k_2 + k_5)$$

The transglucosylation ratio was defined as follows, and was expressed as a function of the substrate concentration using a single parameter:

$$\text{Transglucosylation ratio (\%)} = v_{tg}/v_{ag} \times 100 = [S]/(K_{TG} + [S]) \times 100 \tag{4}$$

where K_{TG} was defined as follows:

$$K_{TG} = k_{cat1}K_{m2}/k_{cat2}$$

The K_{TG} constant is the substrate concentration that gives a transglucosylation ratio of 50%.

Thermal denaturation of the enzyme. An enzyme solution (750 µL), composed of 1.4 nM SmDG, 0.033% BSA, 2 mM EDTA, 0–30 mM $CaCl_2$, and 67 mM sodium acetate buffer (pH 6.0), was incubated at 319 K (46 °C). An aliquot of 40 µL was withdrawn at indicated time and cooled on ice. The residual pNPG-hydrolyzing activity of the aliquot was measured by the standard assay.

pH stability. An enzyme solution (100 µL), composed of 2.1 nM SmDG, 0.01% BSA, 0.6 mM EDTA (or 5 mM $CaCl_2$), and 90 mM sodium acetate buffer (pH 3.6–6.2) or 90 mM Hepes buffer (pH 6.5–

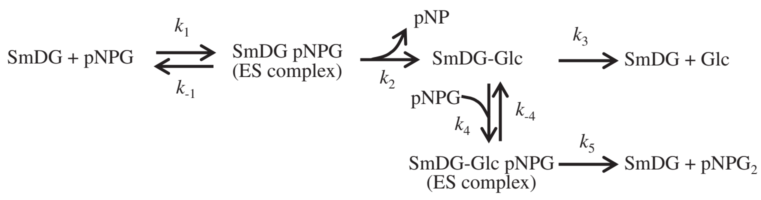

Fig. 2. Kinetic Scheme for the Reaction Catalyzed by SmDG.

SmDG-Glc represents the glucosyl-enzyme intermediate. $pNPG_2$ is *p*-nitrophenyl isomaltoside.

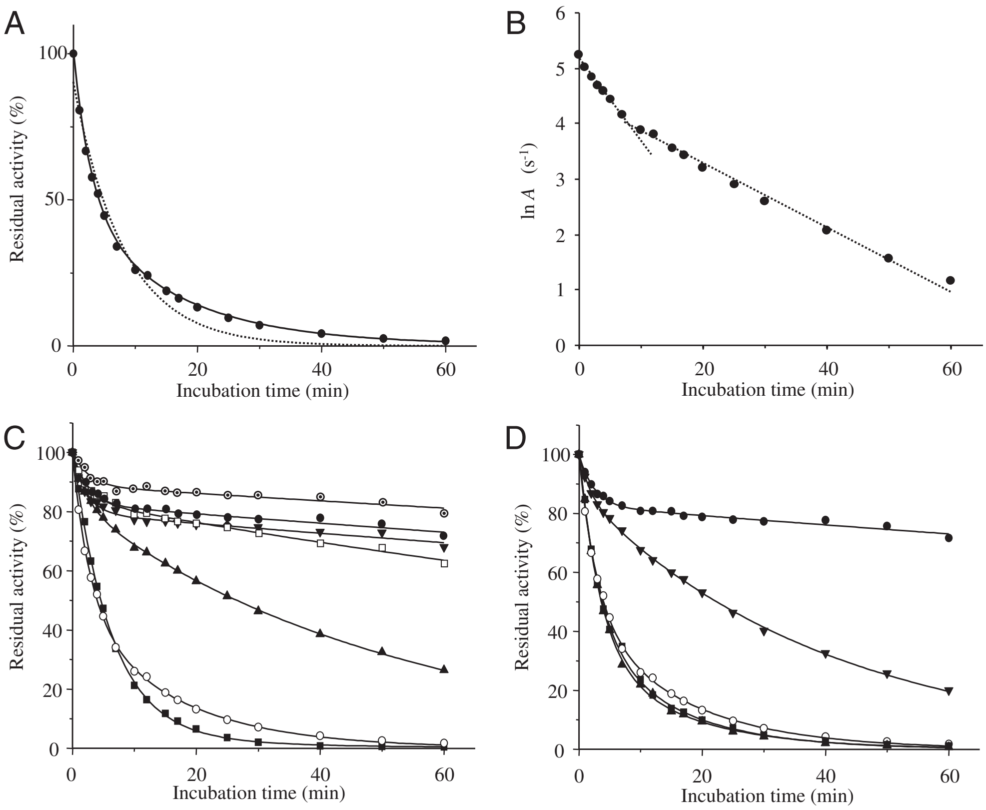

Fig. 3. Time-Dependent Heat Inactivation of SmDG at 46 °C.

A, SmDG of 1.4 nM was incubated at 46 °C in 2 mM EDTA without the addition of $CaCl_2$ and cooled on ice at the indicated times, and the residual activity was measured. The plots of residual activity *versus* incubation time did not follow the theoretical line based on the single-step denaturation model (Eq. (5), broken line), but fitted the two-step irreversible denaturation model (Eq. (6), solid line). B, Semi-logarithmic plots of residual activity (s^{-1}) *versus* incubation time. C, Effects of various concentrations of $CaCl_2$: 0 mM (○), 1 mM (■), 2 mM (▲), 3 mM (□), 5 mM (circled dot), 15 mM (●), and 30 mM (▼). D, Effects of various kinds of salt at 15 mM: KCl (▲), NaCl (■), $MgCl_2$ (▼), and $CaCl_2$ (●), and the absence of any salt as control (○). Residual activities were measured and plotted against incubation times. The fit is to the expression for the two-step irreversible model (Eq. (6)).

7.9), was incubated for 15 min at 37 °C and cooled on ice. After quick neutralization, residual activity toward 2 mM pNPG was assayed using 10 µL of the enzyme solution under the standard reaction conditions except that 100 mM sodium acetate buffer (pH 6.0) and 0.002% BSA were used. The pH range in which SmDG retained more than 90% of the original activity was considered to be the stable range.

Thermal denaturation kinetics. When a fully-active native enzyme (N) undergoes the single-step irreversible thermal deactivation process and is converted directly into a completely inactive form (D),

$$N \rightarrow D$$

the residual activity (A) is expressed as follows:

$$A = A_1 \exp(-k_d t) \qquad (5)$$

where A_1 is the original activity of N, k_d is the rate constant of $N \rightarrow D$, and t is the time of the thermal process. When an enzyme undergoes the two-step irreversible thermal deactivation process, which includes one transitional active intermediate X,

$$N \rightarrow X \rightarrow D$$

the residual activity A is expressed by the following equation:[24)]

$$A = \{A_1 - A_2 k_{d1}/(k_{d1} - k_{d2})\} \exp(-k_{d1} t) + A_2 k_{d1}/(k_{d1} - k_{d2}) \exp(-k_{d2} t) \qquad (6)$$

where A_1 and A_2 are the specific activities of N and X, respectively, and k_{d1} and k_{d2} are the rate constants at $N \rightarrow X$ and $X \rightarrow D$, respectively. The parameters were obtained by the non-linear least squares method (the Levenberg-Marquardt algorithm) with Origin 8.1 (OriginLab, Northampton, MA, USA) in the *t-A* plots. Based on the Eyring transition state theory, activation Gibbs energy $\Delta G^{\ddagger}$ was calculated by the following equation:

$$k = (k_B T/h) \exp\{-\Delta G^{\ddagger}/(RT)\} \qquad (7)$$

where k_B, h, R, and T represent the Boltzmann constant (1.381×10^{-23} J·K^{-1}), the Planck constant (6.626×10^{-34} J·s), the gas constant (8.3145 J K^{-1} mol^{-1}), and the absolute temperature 319 K (46 °C), respectively.

Results

Thermal denaturation process for SmDG

SmDG of 1.4 nM was incubated at 46 °C for 60 min. $CaCl_2$ was not added, but 2 mM EDTA was added to exclude the possible effect of contaminated bivalent cations. Residual activity during the heat denaturation process was monitored (Fig. 3A, B). The time-dependent decrease in activity was not well fitted to the theoretical line based on the simple one-step denaturation model (Eq. (5), Fig. 3A). The plots of $\ln A$ *versus* incubation time t were distinctly nonlinear (Fig. 3B), indicating that the denaturation process was not correctly described by the simple one-step model. The theoretical line based on the two-step irreversible denaturation model, however, was well fitted to the plots (Eq. (6), Fig. 3A). Hence, the heat denaturation of SmDG was expressed by the two-step irreversible denaturation model, in which fully active SmDG (N) was inactivated and converted to an inactive form (D) through an irreversible active intermediate (X). By applying the two-step model equation (Eq. (6)), the specific activities A_1 and A_2 of the fully active native form and the irreversible intermediate, respectively, and rate con-

Table 1. Specific Activities, Rate Constants, and $\Delta G^{\ddagger}$ in the Irreversible Two-Step Heat Denaturation Process and Effects of the Presence of Salts

	A_1[a]	A_2[b]	k_{d1}[c]	k_{d2}[d]	$\Delta G^{\ddagger}{}_1$[e]	$\Delta G^{\ddagger}{}_2$[f]
	($\mu mol\ s^{-1}\ \mu mol^{-1}$)		(s^{-1})		($kJ\ mol^{-1}$)	
no salt[g]	187 ± 1.6	72.6 ± 5.8	0.343 ± 0.028	0.0627 ± 0.0044	81.1	85.7
5 mM $CaCl_2$	181 ± 1.6	159 ± 1.2	0.403 ± 0.075	0.0015 ± 0.00023	80.7	95.6
15 mM $CaCl_2$	189 ± 1.4	155 ± 0.99	0.407 ± 0.042	0.00204 ± 0.00021	80.7	94.7
15 mM $MgCl_2$	199 ± 1.1	165 ± 1.8	0.555 ± 0.066	0.0249 ± 0.00032	79.9	88.1
15 mM KCl	192 ± 1.9	50.2 ± 8.3	0.291 ± 0.026	0.0669 ± 0.0093	81.6	85.5
15 mM NaCl	191 ± 2.1	60.7 ± 10	0.310 ± 0.037	0.0722 ± 0.0096	81.4	85.3

[a]A_1, pNP-releasing activity from 2 mM pNPG of the native form (N) of SmDG.
[b]A_2, the same as A_1, but of the intermediate (X) of SmDG.
[c,d]k_{d1} and k_{d2}, the rate constant of irreversible denaturation step from N to X and from X to the inactive denatured form (D) of SmDG, respectively.
[e,f]$\Delta G^{\ddagger}{}_1$ and $\Delta G^{\ddagger}{}_2$, Gibbs's free energy required for steps of N to X, and X to D, respectively.
[g]Heat denaturation was done in the presence of 2 mM EDTA.

stants k_{d1} and k_{d2} of the irreversible change from N to X and X to D, respectively, were obtained (Table 1). Without any additional salts, the specific activity of the native form ($A_1 = 187\ s^{-1}$) was almost identical to the specific activity ($188 \pm 2.2\ s^{-1}$) of intact SmDG. The specific activity of the intermediate ($A_2 = 72.6\ s^{-1}$) was 39% of A_1. The rate constant of k_{d1} was approximately 5 times higher than k_{d2}. Changes in Gibbs's free energy, $\Delta G^{\ddagger}{}_1$ and $\Delta G^{\ddagger}{}_2$ for inactivation processes N $\rightarrow$ X and X $\rightarrow$ D, respectively, were calculated to be $81.1\ kJ\ mol^{-1}$ and $85.7\ kJ\ mol^{-1}$ at 319 K (46 °C) by Eq. (7) (Table 1).

Effects of Ca^{2+} on the stability of SmDG

Next, the thermostability of SmDG was assayed at the same temperature, 46 °C, but in the presence of $CaCl_2$ at 0–30 mM (Fig. 3C). The activity decreased during incubation at all $CaCl_2$ concentrations, but the rates of denaturation were drastically different depending on the $CaCl_2$ concentration. The activity dropped to 50% in 5 min at 0–1 mM $CaCl_2$, but the presence of 2 mM $CaCl_2$ prolonged this to 30 min, and 3–30 mM $CaCl_2$ stabilized SmDG so that it retained 70% activity or higher even after 60 min of incubation. The most positive effect on stability was obtained at 5 mM $CaCl_2$. All of the time-courses of decrease in residual activity were expressed well by the two-step denaturation model (Eq. (6), Fig. 3C). By fitting the data to Eq. (6), the specific activities, A_1 and A_2, and the rate constants of denaturation, k_{d1} and k_{d2}, were obtained (Table 1). Regardless of the $CaCl_2$ concentration in the thermal process, the specific activity of N (A_1) was in a good agreement with that of intact SmDG. The rate constant from N to X (k_{d1}) was not significantly affected by the addition of 5 or 15 mM $CaCl_2$ either ($k_{d1} = 0.403$ and $0.407\ s^{-1}$, respectively). In contrast, the specific activity of the irreversible intermediate (A_2) was increased 2-fold ($A_2 = 159$ and $155\ s^{-1}$, respectively) and the rate constant toward the completely denatured form, k_{d2}, was decreased 42-fold by the addition of 5 mM $CaCl_2$ ($k_{d2} = 0.0015\ s^{-1}$). The effect of the presence of 15 mM $CaCl_2$ on $\Delta G^{\ddagger}{}_1$ at the first denaturation step was very limited, but $\Delta G^{\ddagger}{}_2$ at the second step was increased by approximately $10\ kJ\ mol^{-1}$. The results indicate that the intermediate was protected by $CaCl_2$ from irreversible denaturation toward the completely inactive form, and the intermediate itself possessed higher activity.

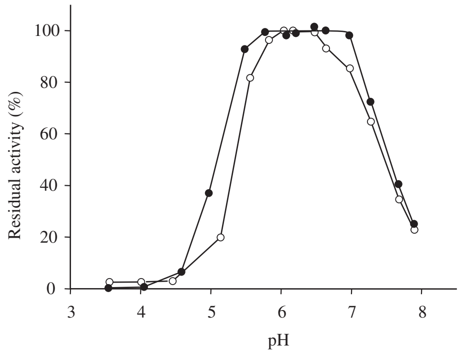

Fig. 4. Effect of $CaCl_2$ on the pH Stability of SmDG.
SmDG of 2.1 nM was incubated at various pH values at 37 °C for 15 min in the absence and the presence of 5 mM $CaCl_2$, and residual activity was measured. SmDG was stable at pH 5.8–6.7 without $CaCl_2$ (○) and at pH 5.5–7.0 with 5 mM $CaCl_2$ (●).

The presence of $CaCl_2$ also affected the pH stability of SmDG (Fig. 4). Without $CaCl_2$, SmDG retained its activity in a narrow pH range (pH 5.8–6.7) after 15 min of incubation at 37 °C. The range was, however, broadened by addition of 5 mM $CaCl_2$, to pH 5.5–7.0.

Effects of other cations on the thermostability of SmDG

The thermal denaturation kinetics at 46 °C of SmDG were analyzed in the presence of other salts: 15 mM KCl, NaCl, and $MgCl_2$ (Fig. 3D). KCl and NaCl did not significantly affect the time-dependent decrease in activity, and hence the kinetic parameters were similar to those without salt (Table 1). The presence of $MgCl_2$, however, decreased the rate of inactivation of SmDG, although the positive effects on the thermostability of SmDG was lower than those due to 15 mM $CaCl_2$ (Fig. 3D, Table 1). In the presence of 15 mM $MgCl_2$, k_{d1} even increased slightly, but k_{d2} dropped to 40%, and A_2 rose to 230% (Table 1).

Kinetics of the catalytic reaction

SmDG catalyzes hydrolysis and transglucosylation simultaneously. The catalytic reaction of SmDG for pNPG was analyzed kinetically. The initial velocities of liberation of pNP (v_{pNP}) and glucose (v_{Glc}) from 0.2–12 mM pNPG were measured. Since aglycone (pNP) is produced by both hydrolysis and transglucosylation, v_{pNP} must be the sum of the velocities of hydrolysis and transglucosylation. v_{Glc} represents hydrolysis, and the

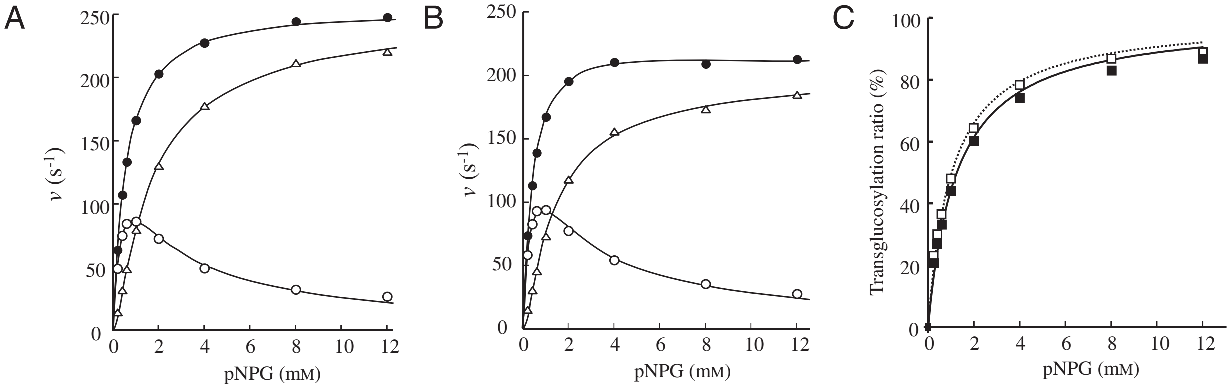

Fig. 5. Kinetics of Catalytic Reaction and the Effect of $CaCl_2$ on Activity.

A and B, The dependence of initial velocities of aglycone release (●), hydrolysis (○), and transglucosylation (hollow triangle) on the pNPG concentration was analyzed in the absence (A) and the presence (B) of 15 mM $CaCl_2$. C, Plots of the transglucosylation ratio *versus* the pNPG concentration in the absence of $CaCl_2$ (□) and the presence of 15 mM $CaCl_2$ (■). The data fitted the theoretical lines well.

Table 2. Kinetic Parameters of SmDG in the Catalytic Reaction on pNPG in the Absence and the Presence of $CaCl_2$

$CaCl_2$	k_{cat1} (s^{-1})	k_{cat2} (s^{-1})	K_{m1} (mM)	K_{m2} (mM)	K_{TG} (mM)
0 mM	173 ± 20	255 ± 3.8	0.288 ± 0.066	1.65 ± 0.12	1.03 ± 0.065
15 mM	175 ± 13	205 ± 4.4	0.366 ± 0.054	1.27 ± 0.16	1.26 ± 0.087

difference (v_{pNP}-v_{Glc}) indicates the transglucosylation velocity. By the reaction scheme shown in Fig. 2 and steady-state kinetics, the initial velocities of hydrolysis, transglucosylation, and the both reactions are expressed by Eq. (2), Eq. (3), and Eq. (1), respectively. In Fig. 5A, the velocities in the absence of $CaCl_2$ are plotted as a function of the pNPG concentration. The velocities of aglycone-release and transglucosylation increased with the pNPG concentration, but the hydrolysis rates reached a maximum at 1 mM pNPG, and decreased with increase in the pNPG concentration. The data fitted the theoretical curves well (Fig. 5A), and the kinetic parameters, k_{cat1}, k_{cat2}, K_{m1}, and K_{m2}, were determined from the theoretical equations (Table 2). The plots of transglucosylation ratios, defined by Eq. (4), *versus* the pNPG concentrations fitted the theoretical saturation curve as well (Fig. 5C, solid squares). The transglucosylation parameter, K_{TG}, the substrate concentration giving a transglucosylation ratio of 50%, was determined to be 1.0 mM (Table 2). The addition of 15 mM $CaCl_2$ did not have a strong impact on the kinetic behavior of the reaction on pNPG (Fig. 5B, C). None of the parameters was significantly different from those in the absence of $CaCl_2$, but the maximum aglycone-releasing velocity, k_{cat2}, decreased 20%, and transglucosylation fell with 20% increased K_{TG} (Table 2).

Discussion

SmDG is a GH13_31 enzyme that has a calcium ion bound to the $\beta \rightarrow \alpha$ loop 1 of the core $(\beta/\alpha)_8$ barrel in the solved three-dimensional structures (Fig. 1).[12] The calcium ion is coordinated in the site by eight atoms from five amino acid residues and two water molecules. The crystal structures of SmDG hold two other calcium ions between symmetry-related enzyme molecules. The crystal used in structural analysis was, however, grown in the presence of a high concentration (200 mM) of calcium chloride, and the two calcium ions were not predicted to be held in the protein molecule in a solution with a low concentration of $CaCl_2$, but were predicted to be released. On the other hand, the other calcium ion on the $\beta \rightarrow \alpha$ loop 1 was predicted to be held in the protein due to tight binding.

Our biochemical analyses of SmDG revealed the function of the calcium ion in enhancing the stability of SmDG. In the absence and the presence of $CaCl_2$, the denaturation kinetics of SmDG were not described by a single exponential decay, but by the two-step irreversible denaturation model, which was used to describe the deactivation of *B. licheniformis* α-amylase[24] and several other enzymes.[25,26] The model postulates that a fully active native enzyme (N) is transformed into a completely inactive form (D) *via* an active intermediate (X) through two irreversible steps. The deactivation intermediate of SmDG in the absence of any additional salt retained 39% of the activity of intact SmDG. In terms of rate constants, the change from N to X was 5.5-fold faster than the second step, from X to D, in the deactivation of SmDG. The addition of divalent cations in the thermal process did not cause a significant difference in the specific activity of N, but enhanced the thermostability of SmDG through an increase in the specific activity of the intermediate and the reduction of k_{d2}, while k_{d1} increased slightly. In the case of 5 mM $CaCl_2$, the specific activity of X increased 2.2-fold, and k_{d2} fell 42-fold. Therefore, according to the model of two-step irreversible denaturation, the effect of calcium ions on the stability of SmDG during the thermal process is achieved by increased specific activity and enhanced stability of the deactivation intermediate.

The thermostability of SmDG was increased by $MgCl_2$ as well, but not by NaCl or KCl, which rather decreased the residual activity (Fig. 3D). Therefore, the enhanced stability was due to the influence of the divalent cations, particularly the calcium ion. On the

Table 3. Amino Acid Sequences of the $\beta \rightarrow \alpha$ Loop 1 Calcium-Binding Site of Structure-Solved GH13 Enzymes

Subfamily	Enzyme	Organism	Calcium-binding site[a]		Ref.
31	Dextran glucosidase (SmDG)	*Streptococcus mutans* ATCC 25175	21	DtNgDgIgD	12
31	Trehalulose synthase (MutB)	*Pseudomonas mesoacidophila* MX-45	49	DtNgDgIgD	13
36	α-Amylase A	*Halothermothrix orenii*	44	DsDgDgIgD	14
unclassified	α-Glucosidase (GSJ)	*Geobacillus* sp. HTA-462	21	DaNgDgIgD	15
unclassified	α-Amylase (SusG)[b]	*Bacteroides thetaiotaomicron* VPI-5482	73	DsDgDgYgD	16
unclassified	4-α-Glucanotransferase (TM0364)	*Thermotoga maritima* MSB8	13	DgNlDgVgD	17
unclassified	Oligo-α-1,6-glucosidase	*Saccharomyces cerevisiae* S288C	30	DsNdDgWgD	18
2	β-Cyclodextrin glucanotransferase	*Bacillus circulans* 251	54	DgNpaNN-(17)-GgD	19
2	Maltogenic α-amylase	*Geobacillus stearothermophilus* C599	54	DgDttNN-(20)-GgD	20
20	Neopullulanase	*Geobacillus stearothermophilus* TRS40	147	NgNpsiS-(18)-GgD	21
20	α-Amylase 2 (TVAII)	*Thermoactinomyces vulgaris* R-47	143	NgDpsND-(19)-GgD	22
unclassified	Cyclomaltodextrinase	*Flavobacterium* sp. 92	137	NgDpsND-(18)-GgD	23
unclassified	α-Amylase 1 (TVA I)	*Thermoactinomyces vulgaris* R-47	174	NgDssND-(35)-GgD	22

[a]Capital letters indicate residues involved in Ca^{2+} binding. Parenthetic numbers in the sequence show numbers between residues.
[b]Mg^{2+} is a ligand.

other hand, chloride ions and the ionic strength of the solution might reduce the thermostability of SmDG. The slight decrease in thermostability with $CaCl_2$ at higher than 5 mM might have been caused in the same way.

It can be assumed that the enhancement of thermostability due to the addition of calcium ions at a low concentration is related to the tight binding of a calcium ion in the $\beta \rightarrow \alpha$ loop 1. The position of calcium binding in the SmDG structure is distinctly different from that commonly found in α-amylases, which often possess Ca^{2+} in domain B (a long protruding loop connecting β3 and α3 in the $(\beta/\alpha)_8$ barrel) maintaining its structural integrity.[7] The predominant α-amylases have no calcium ion in the equivalent position in $\beta \rightarrow \alpha$ loop 1, as observed for SmDG, but calcium binding to the site in loop 1 has been found in many GH13 enzymes (representative examples are listed in Table 3). Even so, little has been known about functions of the calcium ion in that position to date. In cyclodextrin glucanotransferase and cyclodextrinase, which contain a calcium ion in loop 1 in the solved structures, the addition of a chelating reagent such as EDTA or ethyleneglycol bis(2-aminoethylether) tetraacetic acid reduced protein stability,[8,10,22] but it was unclear whether that effect was due to removal of the equivalent calcium ion in loop 1 or another, because the enzymes held two or more calcium ions in a protein molecule. A cyclodextrinase, so-called α-amylase 2 of *T. vulgaris*, is the sole evidence that the calcium ion in the loop 1 is related to increases in the thermostability of the enzyme, because the enzyme holds just one equivalent calcium ion per protein molecule, and chelation with ethyleneglycol bis(2-aminoethylether) tetraacetic acid resulted in a reduction in the thermostability by approximately 5 °C under the experimental conditions.[22] Our results for SmDG provide even more precise evidence as to what positive effects the calcium ion has on the stability of the protein.

As shown in Table 3, the calcium ion-holding loop 1 structures fall into two groups: a short-loop group sharing consensus sequence Dx(N/D/T/S)xDg(I/X)gD, and a long-loop group sharing (D/N)g(D/N)xx(N/x)(N/D/S) and GgD connected with long toes of loop 1, where the capital letters indicate residues involved in direct interaction with the calcium ion, and x denotes any residue. SmDG belongs to the first short-loop group. The consensus sequences are widely distributed in many GH13 enzymes. The first consensus sequence of the short-loop group is shared by GH13 enzymes belonging to subfamilies 16, 17, 23, 29, 30, 31, 35, and 36. The second long-loop group is comprised of GH13 enzymes of subfamilies 2, 19, 20, and 22. Exceptions are found only in subfamily 20. The both sequences are also shared by other GH13 enzymes not yet classified into any subfamily. It has not been known yet whether an equivalent calcium ion is held in the loop 1 site in many of the enzymes. Some solved three-dimensional structures, for instance, oligo-1,6-glucosidase from *Bacillus cereus*,[31] possess no calcium ion as ligand in the loop 1 site in spite of a shared consensus sequence, but it might happen because of the crystal conditions. There is possibility that by the addition of calcium ions to some concentration to the protein solution, calcium ions can be introduced into the calcium-binding site in $\beta \rightarrow \alpha$ loop 1, resulting in an increase in the stability of the enzyme, as observed for SmDG.

Acknowledgment

We thank Mr. Tomohiro Hirose of the Instrumental Analysis Division, Equipment Management Center, Creative Research Institution, Hokkaido University, for amino acid analysis.

References

1) Russell RR and Ferretti JJ, *J. Gen. Microbiol.*, **136**, 803–810 (1990).
2) Saburi W, Mori H, Saito S, Okuyama M, and Kimura A, *Biochim. Biophys. Acta*, **1764**, 688–698 (2006).
3) Cantarel BL, Coutinho PM, Rancurel C, Bernard T, Lombard V, and Henrissat B, *Nucleic Acids Res.*, **37**, D233–D238 (2009).
4) MacGregor EA, Janecek S, and Svensson B, *Biochim. Biophys. Acta*, **1546**, 1–20 (2001).
5) Stam MR, Danchin EG, Rancurel C, Coutinho PM, and Henrissat B, *Protein Eng. Des. Sel.*, **19**, 555–562 (2006).
6) Vallee BL, Stein EA, Sumerwell WN, and Fischer EH, *J. Biol. Chem.*, **234**, 2901–2905 (1959).
7) Machius M, Declerck N, Huber R, and Wiegand G, *Structure*, **6**, 281–292 (1998).
8) Thiemann V, Dönges C, Prowe SG, Sterner R, and Antranikian G, *Arch. Microbiol.*, **182**, 226–235 (2004).
9) Kelly RM, Dijkhuizen L, and Leemhuis H, *Appl. Microbiol. Biotechnol.*, **84**, 119–133 (2009).
10) Kim TJ, Shin JH, Oh JH, Kim MJ, Lee SB, Ryu S, Kwon K,

Kim JW, Choi EH, Robyt JF, and Park KH, *Arch. Biochem. Biophys.*, **353**, 221–227 (1998).
11) Plant AR, Parratt S, Daniel RM, and Morgan HW, *Biochem. J.*, **1**, 865–868 (1988).
12) Hondoh H, Saburi W, Mori H, Okuyama M, Nakada T, Matsuura Y, and Kimura A, *J. Mol. Biol.*, **378**, 913–922 (2008).
13) Ravaud S, Robert X, Watzlawick H, Haser R, Mattes R, and Aghajari N, *J. Biol. Chem.*, **282**, 28126–28136 (2007).
14) Sivakumar N, Li N, Tang JW, Patel BK, and Swaminathan K, *FEBS Lett.*, **580**, 2646–2652 (2006).
15) Shirai T, Hung VS, Morinaka K, Kobayashi T, and Ito S, *Proteins*, **73**, 126–133 (2008).
16) Koropatkin NM and Smith TJ, *Structure*, **18**, 200–215 (2010).
17) Roujeinikova A, Raasch C, Sedelnikova S, Liebl W, and Rice DW, *J. Mol. Biol.*, **321**, 149–162 (2002).
18) Yamamoto K, Miyake H, Kusunoki M, and Osaki S, *FEBS J.*, **277**, 4205–4214 (2010).
19) Lawson CL, van Montfort R, Strokopytov B, Rozeboom HJ, Kalk KH, de Vries GE, Penninga D, Dijkhuizen L, and Dijkstra BW, *J. Mol. Biol.*, **236**, 590–600 (1994).
20) Dauter Z, Dauter M, Brzozowski AM, Christensen S, Borchert TV, Beier L, Wilson KS, and Davies GJ, *Biochemistry*, **38**, 8385–8392 (1999).
21) Hondoh H, Kuriki T, and Matsuura Y, *J. Mol. Biol.*, **326**, 177–188 (2003).
22) Kamitori S, Abe A, Ohtaki A, Kaji A, Tonozuka T, and Sakano Y, *J. Mol. Biol.*, **318**, 443–453 (2002).
23) Fritzsche HB, Schwede T, and Schulz GE, *Eur. J. Biochem.*, **270**, 2332–2341 (2003).
24) Violet M and Meunier JC, *Biochem. J.*, **263**, 665–670 (1989).
25) Henley JP and Sadana A, *Enzyme Microb. Technol.*, **7**, 50–60 (1985).
26) Nury S, Meunier JC, and Mouranche A, *Eur. J. Biochem.*, **180**, 161–166 (1989).
27) Moore S and Stein WH, *J. Biol. Chem.*, **176**, 367–388 (1948).
28) Miwa I, Okudo J, Maeda K, and Okuda G, *Clin. Chim. Acta*, **37**, 538–540 (1972).
29) Brumer H III, Sims PF, and Sinnott ML, *Biochem. J.*, **339**, 43–53 (1999).
30) Kawai R, Igarashi K, Kitaoka M, Ishii T, and Samejima M, *Carbohydr. Res.*, **339**, 2851–2857 (2004).
31) Watanabe K, Hata Y, Kizaki H, Katsube Y, and Suzuki Y, *J. Mol. Biol.*, **269**, 142–153 (1997).